

Two-dimensional subwavelength plasmonic lattice solitons

F. Ye,^{1,5} D. Mihalache,² B. Hu,^{3,5} and N. C. Panoiu⁴

¹*Department of Physics, Shanghai Jiao Tong University, Shanghai 200240, China*

²*”Horia Hulubei” National Institute for Physics and Nuclear Engineering, Department of Theoretical Physics, 407 Atomistilor, Magurele-Bucharest, 077125, Romania*

³*Department of Physics, University of Houston, Houston, Texas 77204-5005, USA*

⁴*Department of Electronic and Electrical Engineering, University College London, Torrington Place, London WC1E 7JE, UK*

⁵*Centre for Nonlinear Studies, and The Beijing-Hong Kong-Singapore Joint Centre for Nonlinear and Complex Systems (Hong Kong), Hong Kong Baptist University, Kowloon Tong, Hong Kong, China*

We present a theoretical study of plasmonic lattice solitons (PLSs) formed in two-dimensional (2D) arrays of metallic nanowires embedded into a nonlinear medium with Kerr nonlinearity. We analyze two classes of 2D PLSs families, namely, fundamental and vortical PLSs in both focusing and defocusing media. Their existence, stability, and subwavelength spatial confinement are studied in detail. © 2018 Optical Society of America

OCIS codes: 190.6135, 240.6680.

When the size of photonic systems is reduced to subwavelength scale, the light confinement and propagation are severely limited by diffraction. Overcoming this major challenge of confining and manipulating optical energy at the nanoscale has attracted a rapidly growing interest in nanophotonics [1]. To this end, one promising approach employs surface plasmon polaritons (SPPs) of metallo-dielectric nanostructures [2]. Although most of the experimental and theoretical studies of SPPs have focused on their linear optical features, there is a growing interest in the optical properties of SPPs in the nonlinear regime [3–7]. This is primarily because the strong enhancement of the optical field induced by the excitation of SPPs can significantly boost nonlinear optical effects, as well as the promising applications of nonlinear SPPs in the all-optical control at nanoscale. A new approach to achieve subwavelength confinement and control of the optical field, employing one-dimensional (1D) arrays of parallel metallic nanowires embedded in an optical medium with Kerr nonlinearity, was

recently proposed [6]. Under certain conditions the optical nonlinearity induced by SPPs field exactly balances the discrete diffraction in the plasmonic array, and as such collective excitation of 1D *plasmonic lattice solitons* (PLSs), are formed in the array. Because the radius a of the nanowires and their separation distance d , are much smaller than the operating wavelength λ , the spatial width of the PLSs can be significantly smaller than λ .

In this Letter, we study the nonlinear optical modes in 2D arrays of metallic nanowires which are embedded into a Kerr medium [Fig. 1(a)]. We found that 2D PLSs of subwavelength spatial extent in the transverse section could exist in this geometry. In addition to the fundamental PLSs, 2D plasmonic arrays support vortical solitons, i.e., solitons with an internal topological phase change of 2π along a closed contour around soliton's phase singularity. The vortical PLSs can also be of subwavelength extent. Fundamental and vortical PLSs are found to exist in both focusing and defocusing media.

Our analysis is an extension of the coupled mode theory developed in Ref. [6] for 1D coupled metallic nanowires. Briefly, the total electric and magnetic fields are expanded as a superposition of the modes of a single nanowire (assumed to have only the fundamental TM mode), and using the conjugated form of the Lorentz reciprocity theorem one obtains

$$\begin{aligned}
 i\frac{d\phi_{m,n}}{dz} + \kappa(\phi_{m,n+1} + \phi_{m,n-1} + \phi_{m+1,n} + \phi_{m-1,n}) + \\
 \mu(\phi_{m+1,n+1} + \phi_{m+1,n-1} + \phi_{m-1,n+1} + \phi_{m-1,n-1}) + \\
 \gamma|\phi_{m,n}|^2\phi_{m,n} = 0,
 \end{aligned} \tag{1}$$

where z is the longitudinal coordinate, $\phi_{m,n}$ is the normalized mode amplitude in nanowire (m, n) , κ and μ are the coupling coefficients between neighboring and next-neighboring nanowires, respectively, and γ is the normalized nonlinearity coefficient. Note that $\gamma > 0$ ($\gamma < 0$) for a medium with self-focusing (self-defocusing) Kerr response. We emphasize that, unlike in the case of conventional dielectric waveguides, for our plasmonic array, $\kappa < 0$, $\mu < 0$, so that the linear dispersion, $k_z = 2\kappa[\cos(k_x d) + \cos(k_y d)] + 4\mu\cos(k_x d)\cos(k_y d)$, forms a concave surface with anomalous diffraction occurring at the Γ point ($k_x = k_y = 0$), while normal diffraction at the M points ($k_x = k_y = \pm\pi/d$) [Fig. 1(b)].

The soliton solution to Eq. (1) are sought in the form $\phi_{m,n}(z) = u_{m,n} \exp(i\beta\kappa z)$, where the amplitudes $u_{m,n}$ are independent of z and β is the soliton wave number (normalized by κ). The soliton is characterized by its power $P = \sum_{m,n} |\phi_{m,n}|^2$. This *ansatz* is inserted into Eq. (1) and the resulting system of equations is solved numerically by a standard relaxation method. The corresponding amplitudes are then used to reconstruct the fields of the PLSs. To quantify the transverse size of solitons we use the effective radius, $R = (\int\int_{-\infty}^{\infty} |\mathbf{E}|^2 [(x - x_0)^2 + (y - y_0)^2] dx dy / \int\int_{-\infty}^{\infty} |\mathbf{E}|^2 dx dy)^{1/2}$, where $(x_0, y_0) = \int\int_{-\infty}^{\infty} (x, y) |\mathbf{E}|^2 dx dy / \int\int_{-\infty}^{\infty} |\mathbf{E}|^2 dx dy$ is the mean center position. In the analysis below, we assumed that the nanowires are made of Ag and used the Drude model, $\epsilon_m(\omega) = 1 - \frac{\omega_p^2}{\omega(\omega + i\nu)}$, for the permittivity of the metal. For

Ag, $\omega_p = 13.7 \times 10^{15}$ rad/s and $\nu = 2.7 \times 10^{13}$ rad/s. For simplicity, we assume that metal is lossless.

We first search for fundamental solitons. As in the case of the 1D PLSs [6], we also find two types of 2D PLSs, i.e., staggered and unstaggered solitons. In the case of unstaggered (staggered) PLSs the phase difference of the mode amplitude in adjacent nanowires is equal to zero (π). The spatial profile of the amplitude and longitudinal field of unstaggered (staggered) PLSs corresponding to a nonlinear change of $\delta n_{nl} = -0.05$ ($\delta n_{nl} = 0.05$) are shown in Fig. 2(a) and (b) [Fig. 2(c) and (d)]. Importantly, due to the inverted linear dispersion relation, staggered (unstaggered) solitons are formed in self-focusing (self-defocusing) media, which is opposite to the case of dielectric waveguide arrays. Note also that the solitons have subwavelength size, the radius being $R = 0.35\lambda$ [Fig. 2(a,b)] and $R = 0.50\lambda$ [Fig. 2(c,d)]. The dependence of soliton radius on β is shown in Fig. 2(e). The plot shows that both staggered and unstaggered PLSs shrink monotonically as their wave number moves away from the band edges. This is because staggered (unstaggered) PLSs originate from the (extended) Bloch modes at the point M (Γ), and thus when their wave number is close to the band edge, solitons have a large width. A larger change of nonlinear refractive index tunes the soliton mode deeper into the gap [see inset of Fig. 2(e)] and thus PLSs are increasingly smaller than λ . Importantly, our calculations show that the power carried by such PLSs cannot be smaller than a threshold value, as can be seen from Fig. 2(f). The nonmonotonic relationship $P = P(\beta)$ has an important implication on soliton stability, as will be shown below.

In addition to the fundamental PLSs, 2D plasmonic arrays also support a new type of PLSs, which has no counterpart in 1D systems, i.e., vortex PLSs; these belong to the class of *discrete vortices* [8]. Here we focus on off-site vortices, i.e., compact vortex states whose singularity is located between lattice sites. Similarly to fundamental PLSs, vortex PLSs exist both in self-focusing [Fig. 3(a,b)] and self-defocusing media [Fig. 3(c,d)]. As can be easily seen from the phase profiles, the vortex has a topological charge equal to 1 (2D PLSs with topological charge 2 also exist, although not shown in here). Interestingly, the phase profile for PLSs in focusing media features a "staggered" pattern at the sites far away from the soliton center, which is a typical feature of "gap" vortices [9]. However, one should mention that the staggered vortex PLS resides at the semi-infinite gap (above the band) and thus is not a "gap" vortex. This is again a consequence of the inverted linear dispersions. The properties of vortex PLSs are summarized in Fig. 3(e,f). Several differences from fundamental PLSs are observed. First, unlike the fundamental PLSs where their value of β can be very close to the band edges, vortex soliton can only exist in the gaps at a finite distance from the band edges. This is due to the fact that the vortex mode is not a Bloch mode of the linear plasmonic array. Secondly, as vortex PLSs possess four intensity maxima, vortex solitons always have a larger width as compared to that of fundamental ones (under the same change

of nonlinear refractive index). Therefore, forming a subwavelength vortex generally requires stronger nonlinearity. Nevertheless, we find that subwavelength vortex PLSs can be achieved under experimentally accessible conditions. For example, the vortex presented in Fig. 3(a,b) has radius $R = 0.3\lambda$ requiring a nonlinear change of refractive index $\delta n_{nl} = 0.11$. Note that an index change of ~ 0.14 was reported in Ref. [10]. Further, the PLSs size can be significantly reduced if the operating wavelength is scaled down, thus the requirement for a strong nonlinear change of the refractive index can be relaxed. Finally, we mention that as in the case of fundamental solitons, vortex PLSs also feature power thresholds for their formation.

A relevant issue associated with the 2D PLSs is their stability. To address this issue, we integrate Eq. (1) by using the Runge-Kutta method with the input condition being the stationary soliton solution plus random noise. Our extensive simulations show that the fundamental PLSs obey the Vakhitov-Kolokolov stability criterion namely, staggered (unstaggered) PLSs are stable when $dP/d\beta > 0$ ($dP/d\beta < 0$) and are unstable otherwise. In the stability region, soliton maintains its original shape over a sufficiently long distance while the initial added noise is rapidly eliminated. In contrast, unstable solitons tend to relax to stable ones with the same power and large oscillations are observed during propagation [Fig. 4(a,b,e)]. The vortex can be also stable, although its stability region is more limited. An unstable propagation of vortex PLS is shown in Fig. 4(c,d). The vortex quickly loses its screwed phase structure and decays into a fundamental PLS. Note that the stability domain of vortex PLSs increases at a shorter operating wavelength.

In conclusion, we presented the first study of 2D plasmonic lattice solitons in arrays of metallic nanowires embedded into a host medium with Kerr nonlinearity. Stable subwavelength fundamental and vortex PLSs are found to exist in both focusing and defocusing media. The work of N. C. P. was supported by the EPSRC.

References

1. W. L. Barnes, A. Dereux, and T. W. Ebbesen, "Surface plasmon subwavelength optics," *Nature (London)* **424**, 824 (2003).
2. A. V. Zayats, I. I. Smolyaninov, and A. A. Maradulin, "Nano-optics of surface plasmon polaritons," *Phys. Rep.* **408**, 131 (2005).
3. E. Feigenbaum and M. Orenstein, "Plasmon-soliton," *Opt. Lett.* **32**, 674 (2007).
4. Y. Liu, G. Bartal, D. A. Genov, and X. Zhang, "Sub-wavelength discrete solitons in nonlinear metamaterials," *Phys. Rev. Lett.* **99**, 153901 (2007).
5. A. R. Davoyan, I. V. Shadrivov, and Y. S. Kivshar, "Nonlinear plasmonic slot waveguides," *Opt. Express* **16**, 21209 (2008).

6. F. Ye, D. Mihalache, B. Hu, and N. C. Panoiu, "Subwavelength plasmonic lattice solitons in arrays of metallic nanowires," *Phys. Rev. Lett.* **104**, 106802 (2010).
7. A. Marini, A. V. Gorbach and D. V. Skryabin, "Coupled mode approach to surface plasmon polaritons in nonlinear periodic structures," *Opt. Lett.* xx, xxxxx (2010).
8. B. A. Malomed and P. G. Kevrekidis, "Discrete vortex solitons," *Phys. Rev. E* **64**, 026601 (2001).
9. E. A. Ostrovskaya and Y. S. Kivshar, "Matter-wave gap vortices in optical lattices," *Phys. Rev. Lett.* **93**, 160405 (2004).
10. L. Brzozowski, E. H. Sargent, A. S. Thorpe, and M. Extavour, "Direct measurements of large near-band edge nonlinear index change from 1.48 to 1.55 μm in InGaAs/InAlGaAs multiquantum wells," *Appl. Phys. Lett.* **82**, 4429 (2003).

List of Figures

- | | | |
|---|---|----|
| 1 | (Color online) (a) Schematics of a 2D square array of nanowires with radius a and separation distance d . (b) The band predicted by the coupled mode theory. | 7 |
| 2 | (Color online) The normalized electric field amplitude (a,c) and longitudinal component (b,d) in focusing (top panels) and defocusing (middle panels) media. $\lambda = 1550$ nm, $a = 40$ nm, $d = 8a$. (a,b) $\beta = 3.58$, $\delta n_{\text{nl}} = 0.05$. (c,d) $\beta = -4.89$, $\delta n_{\text{nl}} = -0.05$. Radius R (e) and power P (f) vs β . The solid and dashed lines stand for $d = 7a$ and $d = 8a$, respectively. In inset, δn_{nl} vs β for $d = 8a$, in focusing medium. | 8 |
| 3 | (Color online) The normalized electric field amplitude (a,c) and longitudinal component (b,d) in focusing (top panels) and defocusing (middle panels) nonlinear media. (a,b) $\beta = 3.82$, $\delta n_{\text{nl}} = 0.11$. (c,d) $\beta = -5.2$, $\delta n_{\text{nl}} = -0.18$. Radius R (e) and power P (f) vs normalized eigenvalue β . The solid and dashed lines stand for $d = 7a$ and $d = 8a$, respectively. In inset, δn_{nl} vs β for $d = 8a$, in focusing medium. | 9 |
| 4 | (Color online) Unstable propagation of the fundamental soliton at $\beta = 3.8$ (top panels) and vortex at $\beta = 3.82$ (middle panels), showing the intensity profile at $z = 0$ (a,c), $z = 60$ μm (b), and $z = 90$ μm (d). (e) Variation of maximum amplitude vs propagation distance for fundamental (dashed) and vortex (solid) solitons. | 10 |

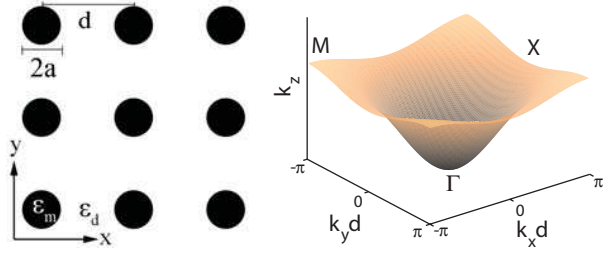


Fig. 1. (Color online) (a) Schematics of a 2D square array of nanowires with radius a and separation distance d . (b) The band predicted by the coupled mode theory.

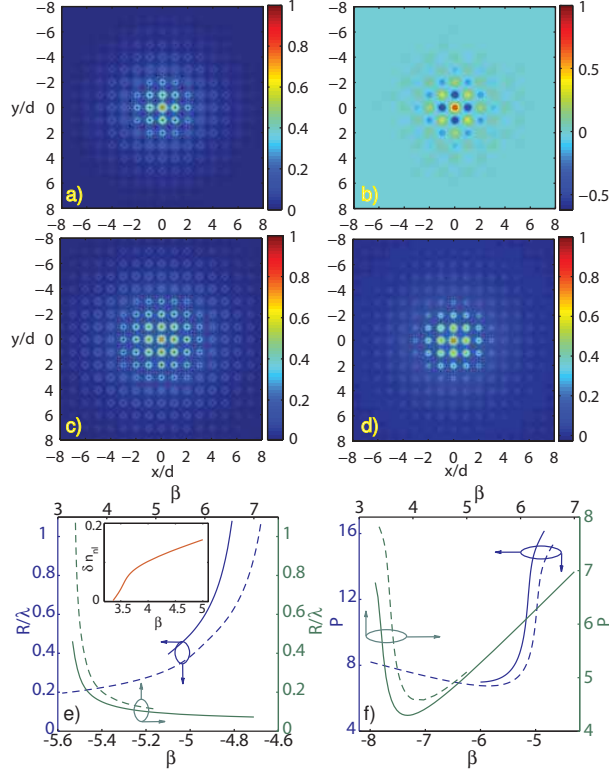


Fig. 2. (Color online) The normalized electric field amplitude (a,c) and longitudinal component (b,d) in focusing (top panels) and defocusing (middle panels) media. $\lambda = 1550$ nm, $a = 40$ nm, $d = 8a$. (a,b) $\beta = 3.58$, $\delta n_{m1} = 0.05$. (c,d) $\beta = -4.89$, $\delta n_{m1} = -0.05$. Radius R (e) and power P (f) vs β . The solid and dashed lines stand for $d = 7a$ and $d = 8a$, respectively. In inset, δn_{m1} vs β for $d = 8a$, in focusing medium.

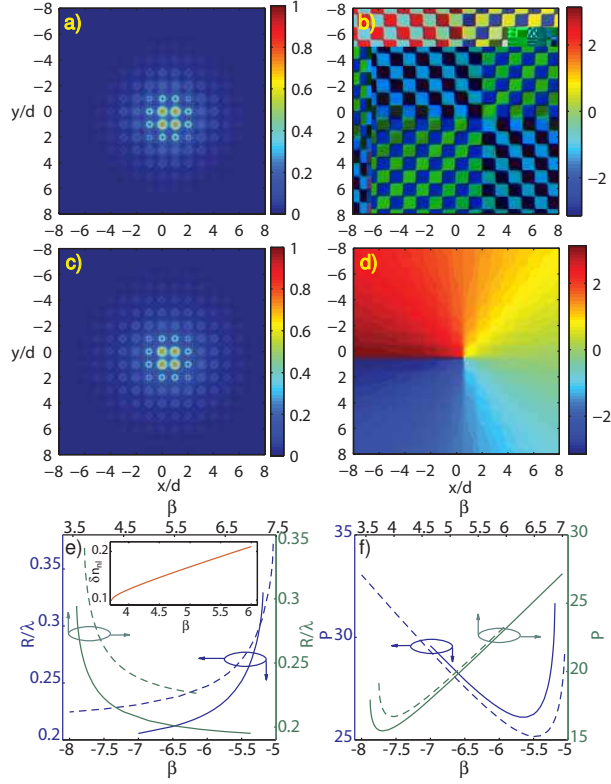


Fig. 3. (Color online) The normalized electric field amplitude (a,c) and longitudinal component (b,d) in focusing (top panels) and defocusing (middle panels) nonlinear media. (a,b) $\beta = 3.82$, $\delta n_{nl} = 0.11$. (c,d) $\beta = -5.2$, $\delta n_{nl} = -0.18$. Radius R (e) and power P (f) vs normalized eigenvalue β . The solid and dashed lines stand for $d = 7a$ and $d = 8a$, respectively. In inset, δn_{nl} vs β for $d = 8a$, in focusing medium.

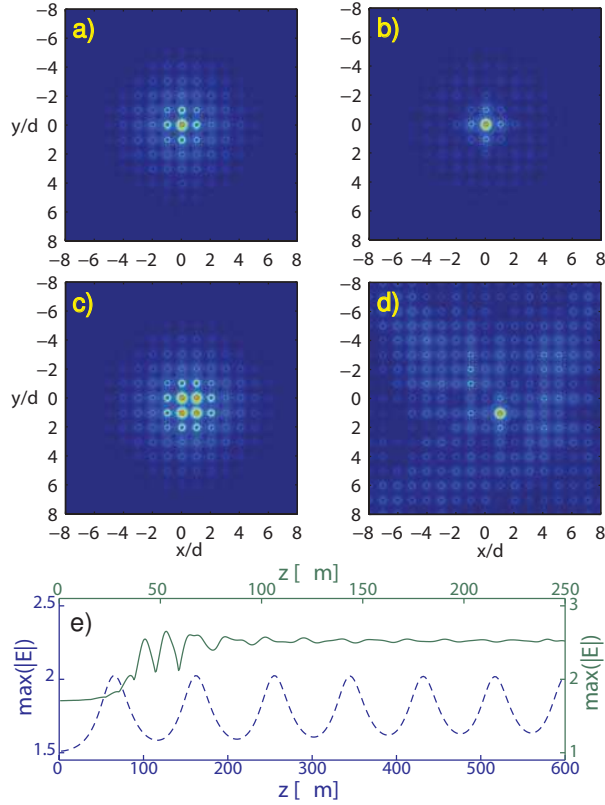


Fig. 4. (Color online) Unstable propagation of the fundamental soliton at $\beta = 3.8$ (top panels) and vortex at $\beta = 3.82$ (middle panels), showing the intensity profile at $z = 0$ (a,c), $z = 60 \mu\text{m}$ (b), and $z = 90 \mu\text{m}$ (d). (e) Variation of maximum amplitude vs propagation distance for fundamental (dashed) and vortex (solid) solitons.